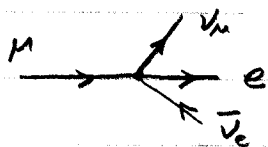
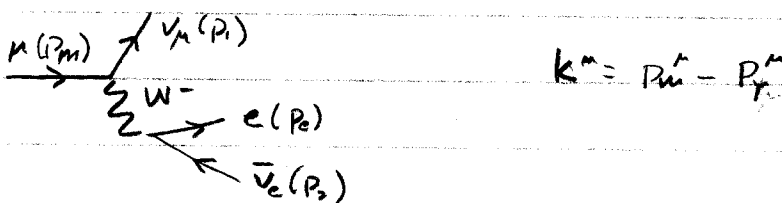


Muon Decay

One of the simplest weak interactions is muon decay, originally thought to be another 4-fermion interaction,



but in the 1950's, thought to be the result of



The utility of this is of 2 sorts. First, it is precisely the ^{semileptonic} decay sequence of quarks lighter than about M_W and second, various new physics scenarios predict the presence of additional gauge groups, which in turn require various additional W and Z bosons. Very precise μ decay measurements are sensitive to such a mixing with the "regular" W^- especially if a RH weak interaction is involved.

The T matrix for the exchange graph is,

$$T = (-i) \left(\frac{ig}{2\sqrt{2}} \right) \left[\bar{u}_\nu \gamma_\mu (1-\gamma_5) u_\mu \right] \left[\frac{g^{\mu\nu} - k^\mu k^\nu / M_W^2}{k^2 - M_W^2} \right] \left(\frac{ig}{2\sqrt{2}} \right) \left[\bar{u}_e \gamma_\nu (1-\gamma_5) v_{\bar{\nu}_e} \right]$$

Certainly, $|k^2| \ll M_W^2$ so,

$$g \frac{k^\mu - k^\mu k^\nu / M_W^2}{k^2 - M_W^2} \rightarrow -\frac{g^{\mu\nu}}{M_W^2}$$

Using the definition

$$\frac{g^2}{8M_W^2} = \frac{G_F}{\sqrt{2}} \quad \text{we}$$

would have the graph for the 1st diagram.

$$T = -i \frac{G_F}{\sqrt{2}} \bar{u}_\mu \gamma_\mu (1-\gamma_5) u_m \bar{u}_e \gamma^\mu (1-\gamma_5) v_{\bar{\nu}_e}$$

The rate will be

$$d\Gamma = (2\pi)^4 \delta(p_e + p_1 + p_2 - p_m) \frac{1}{2E_\mu} \sum |T|^2 d^3P_e d^3P_1 d^3P_2$$

By the usual fermionic techniques,

$$|T|^2 = \frac{1}{2} G_F^2 \sum_{\mu e} \sum_{\nu \bar{\nu}_e} \sum_{\mu} \sum_{\nu} u_\nu \bar{u}_\nu \gamma_\mu (1-\gamma_5) u_m \bar{u}_m \gamma_\nu (1-\gamma_5) \\ \times u_e \bar{u}_e \gamma^\mu (1-\gamma_5) v_{\bar{\nu}_e} \bar{v}_{\bar{\nu}_e} \gamma^\nu (1-\gamma_5)$$

We will not average over initial μ helicities and will not consider outgoing electron helicities.

So, for example we will project out both the
+ energy and helicity electrons--

$$\sum_{i=1}^2 u_e^{(i)} \bar{u}_e^{(i)} = \frac{1}{2} (\not{p}_e + m_e) (1 + \gamma_5 \not{s}_e) \quad \text{ditto for muon}$$

where, remember, in the μ rest frame $S_{\mu} = (0, \hat{s}_{\mu})$

The traces are actually quite involved algebraically,
and we would get,

$$|T|^2 = \frac{1}{2} G_F^2 (\not{p}_e - m_e \not{s}_e) \cdot \not{p}_2 (\not{p}_{\mu} - m_{\mu} \not{s}_{\mu}) \cdot \not{p}_1 \quad \text{4 vectors}$$

The neutrinos will both be undetected, so integrate
them away - with a trick.

Write,

$$d\Gamma = \frac{2G_F^2}{(2\pi)^5} \frac{d^3 p_e}{E_e E_m} (\not{p}_e - m_e \not{s}_e)^{\mu} (\not{p}_{\mu} - m_{\mu} \not{s}_{\mu})^{\nu} I_{\mu\nu}$$

where

$$I_{\mu\nu} \equiv \iint \delta^4(p_1 + p_2 - q) p_{2\mu} p_{1\nu} \frac{d^3 p_1}{E_1} \frac{d^3 p_2}{E_2}$$

Define $q^{\mu} \equiv p_{\mu}^{\mu} - p_e^{\mu} = p_1^{\mu} + p_2^{\mu}$

The only vectors and tensors that $I_{\mu\nu}$ can depend on are q^μ and $g^{\mu\nu}$, so generally parameterize it as,

$$I_{\mu\nu} = A q^2 g_{\mu\nu} + B q_\mu q_\nu$$

Multiply by $g^{\mu\nu}$ and $q^\mu q^\nu$

$$g^{\mu\nu} I_{\mu\nu} = 4Aq^2 + Bq^2 = \iint \frac{\delta(\)}{E_1 E_2} p_1 \cdot p_2 d^3 p_1 d^3 p_2$$

and

$$q^\mu q^\nu I_{\mu\nu} = Aq^4 + Bq^4 = \iint \frac{\delta(\)}{E_1 E_2} (p_1 \cdot p_2)^2 d^3 p_1 d^3 p_2$$

We can evaluate these invariants in any frame,

choose the one in which $\vec{p}_1 = -\vec{p}_2 \Rightarrow q^\mu = (q^0, \vec{0})$.

Then, $\vec{p}_1 + \vec{p}_2 - \vec{q} = 0$ and so $\int \delta^3(0) d^3 p_2 = 1$

So,

$$g^{\mu\nu} I_{\mu\nu} = 8\pi \int E_1^2 dE_1 \delta(2E_1 - q^0) = \pi q^2$$

$$q^\mu q^\nu I_{\mu\nu} = 16\pi \int E_1^4 dE_1 \delta(2E_1 - q^0) = \frac{1}{2} \pi q^2$$

Solving for A & B ..

$$A = \pi/6 \quad \text{and} \quad B = \pi/3$$

$$\vec{p}_1 \cdot \vec{p}_2 = E_1 E_2 - \vec{p}_1 \cdot \vec{p}_2 = 2E_1 E_2 + 2E_1 E_2 = 2E_1 E_2$$

$$d^3 p_1 = p_1^2 dp_1 d\Omega = 4\pi E_1^2 dE_1$$

$$E_1 = E_2 \quad \int \delta(2E_1 - q^0) 4\pi \cdot 2 \cdot E_1 E_2 \frac{E_1^2}{E_1^2} dE_1 = \int (8\pi E_1^2 dE_1 \delta(2E_1 - q^0))$$

$$\delta(2E_1 - q^0) = \frac{1}{2} \delta(E_1 - q^0/2)$$

$$4\pi E_1^2 \Big|_{E_1 = q^0/2}$$

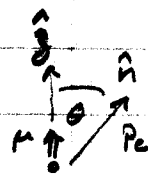
$$4\pi \frac{q^2}{4} = \pi q^2$$

So, $I_{\mu\nu} = \frac{1}{6} \pi (g^2 g_{\mu\nu} + 2g_\mu g_\nu)$

and

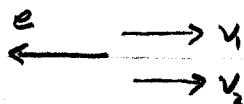
$$dP = \frac{\pi}{3} \frac{G_F^2}{(2\pi)^5} \frac{d^3 p_e}{E_e E_\mu} (p_e - m_e s_e)^\mu (p_\mu - m_\mu s_\mu)^\nu (g^2 g_{\mu\nu} + 2g_\mu g_\nu)$$

Choose μ rest frame and use $m_e \ll m_\mu$. w/

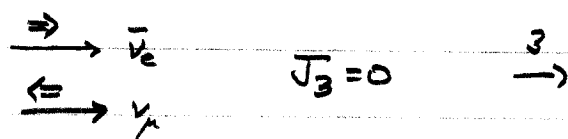


$$dP = \frac{\pi G_F^2}{96 m_\mu} d\Omega_e p_e dE_e (1 - \hat{n} \cdot \hat{s}_e) E_e m_\mu^2 \times [(3m_\mu - 4E_e) + (m_\mu - 4E_e) \hat{n} \cdot \hat{s}_\mu]$$

The maximum electron energy would be when



Because of velocity assignments for neutrinos and antineutrinos



then, at this max E_e configuration, \hat{s}_e and \hat{s}_μ must be related:



In max E_e state,
and

$$E_\mu = E_e^M + 2E_v = m_\mu$$

$$\vec{p}_e^M = 2\vec{p}_v = 2E_v \hat{z}$$

so

$$E_e^M + |\vec{p}_e^M| = m_\mu \quad \checkmark$$

$$E_e^M = m_\mu/2$$

since $m_e \ll m_\mu$

Define

$$x = E_e/E_e^M$$

so

$$E_e = \frac{x m_\mu}{2}$$

and with

$$\hat{s}_m = \hat{z}$$

$$dP = \frac{G_F^2 m_\mu^5}{192\pi^3} \underbrace{[2x^2(3-2x)]}_{\text{I}} \underbrace{[1 + \alpha \cos\theta]}_{\text{II}} \underbrace{\left[\frac{1 - \hat{n} \cdot \hat{s}_e}{2} \right]}_{\text{III}} dx \frac{\sin\theta d\theta dp}{4\pi}$$

asymmetry wrt \hat{s}_m
h(e), helicity of e

where

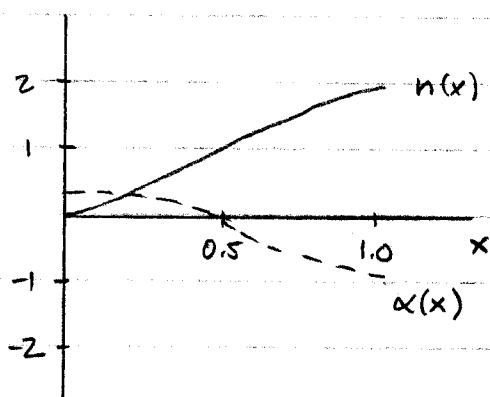
$$\alpha = \frac{1-2x}{3-2x}$$

(= -1 for $x=1$ when

$$E_e = E_e^M)$$

Further, $h(e) = -1$, independent of x .

These normalized quantities have the following energy dependence:



Integrating, the total rate is,

$$P = \frac{G^2 m_\mu^5}{192\pi^3}$$

and an early measured value was $2.2 \times 10^{-6} \text{ s}$ which gave $G_\mu \approx G_F$.

$$\tau = P^{-1}$$

A traditional way to analyze μ decay (and τ and subsequently top) is to parameterize

$$T = \frac{G_F}{\sqrt{2}} \sum_i \bar{u}_e \theta_i u_\mu \bar{\nu}_e \theta_i (C_i + C_i' \gamma_5) \nu_i \quad \text{with } g_i^2 = |C_i|^2 + |C_i'|^2$$

which is rendered into the charge-retention form --

Then, various couplings are formed:

$$\rho = (3g_A^2 + 3g_V^2 + 6g_T^2) / D$$

$$\eta = (g_S^2 - g_P^2 + 2g_A^2 - 2g_V^2) / D$$

$$\xi = (6g_S g_P \cos \phi_{SP} - 8g_A g_V \cos \phi_{AV} + 14g_T^2 \cos \phi_{TT}) / D$$

$$\delta = (-6g_A g_V \cos \phi_{AV} + 6g_T^2 \cos \phi_{TT}) / D$$

$$h = (2g_S g_P \cos \phi_{SP} - 8g_A g_V \cos \phi_{AV} - 6g_T^2 \cos \phi_{TT}) / D$$

$$D = g_S^2 + g_P^2 + 4g_V^2 + 6g_T^2 + 4g_A^2$$

$$\cos \theta_{ij} = \text{Re} (C_i^* C_j' + C_i' C_j^*)$$

collectively called
the Michel Parameters

← often (incorrectly) called
"The Michel Parameter"
or (correctly) "the ρ parameter"

In general, the rate becomes,

$$d\Gamma = \frac{D}{16} \frac{G^2 m_\mu^5}{192\pi^3} \frac{\sin\theta d\theta dp}{4\pi}$$

$$\times \left\{ [12(1-x) + \frac{4}{3}\rho(8x-6)] \right.$$

$$\times \left. \xi \cos\theta [4(1-x) + \frac{4}{3}\delta(8x-6)] \right\} x^2 dx$$

ρ & δ characterize the high end of the β spectrum.

ξ characterizes the asymmetry

η drops out in a massless electron limit

For $V \notin A$

$$\rho = 3/4$$

$$\delta = 3/4$$

$$\xi = \frac{2g_A g_V \cos\phi_{AV}}{g_A^2 + g_V^2}$$

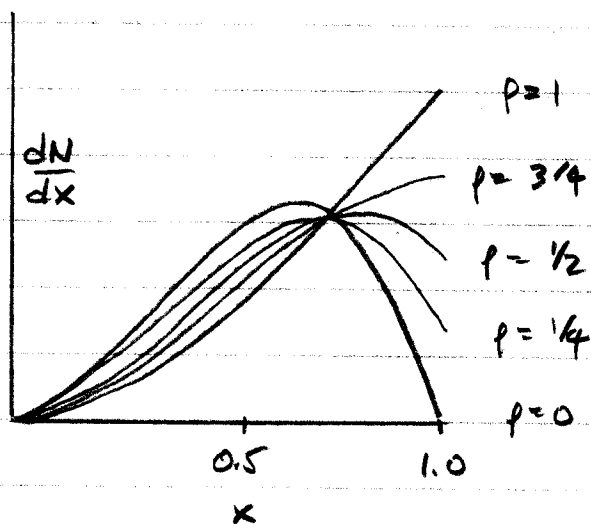
$V-A$

$$\rho = 3/4$$

$$\delta = 3/4$$

$$\xi = -1$$

$$\eta = 0$$



$$\text{Best } \rho = 0.7503 \pm 0.0026$$

Peardor, unpubs.
 $\eta = 0$

$$\rho = 0.7518 \pm 0.0026$$

$$\text{w/ } \eta = -0.12 \pm 0.21$$

in 2 parameter fit

My favorite plot shows the evolution of ρ -- 1957/58 was the $V-A$ prediction. Also shown is a modern measurement.

$$\rho = 0.7518 \pm 0.0026 \quad (3.68)$$

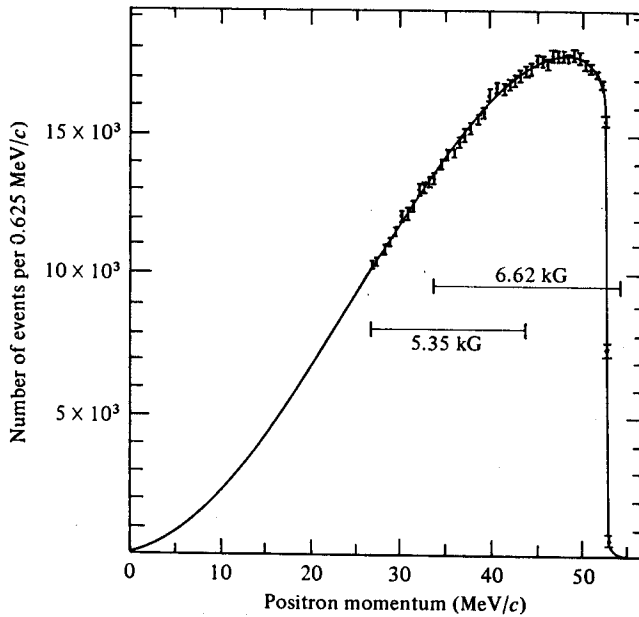
The quantity η , which should be zero according to the V-A law, was measured by stopping π^+ and μ^+ in a bubble chamber in a strong magnetic field. Over 400,000 exposures were taken, including 2,070,000 μ^+ decays. Momentum measurements calibrated with internal conversion e^- tracks of known momentum from a radioactive source inside the bubble chamber yielded (Derenzo 69):

$$\eta = -0.12 \pm 0.21 \quad (3.69)$$

3.4.4 Asymmetry in the decay of polarized muons

The parameter ξ should take the value -1 according to the V-A law, and experimental measurement of ξ is important because observation of departure of ξ from -1 would signify the existence of right-handed (V + A) currents, as expected in left-right symmetric models (see Section 2.12). The experimental problem is very difficult because one actually observes the product $P\xi$, where P is the polariza-

Figure 3.7. Results of experiments to determine ρ . Experimental points are plotted, together with a theoretical curve for $\rho = \frac{2}{3}$ corrected for radiative effects and ionization loss. (From Bardon et al. 65. Reprinted with permission.)



tion of the muons. This quantity is measured because of miscellaneous muon decays which can easily be accounted for by a neglected asymmetry $a = \xi/3$ which is neglected in stopping in photoemulsion in the muon spin. The result (G

$$\xi = -0.972 \pm 0.013$$

was found, in accord with the prediction of the coefficient to constrain left-right symmetry (see Section 2.12). In a measurement of ξ stopped in the magnetic field, the polarization which is used for both momentum and helicity. The parameters δ and P are determined by comparing the results to experimental results. The result (G

$$\delta = 0.7551 \pm 0.0085$$

3.4.5 Summary

Table 3.2 presents the results of the experiments with predictions of the V

Table 3.2. Properties of the muon

Parameter	
Muon mass m_μ	
m_μ/m_e	
ν_μ mass m_{ν_μ}	
Maximum electron energy in muon decay assuming $m_{\nu_e} = m_{\nu_\mu} = 0$	
Muon mean life	
Michel parameters	
ρ	
η	
ξ	
δ	
$h(e^-)$	

* At 90% confidence level

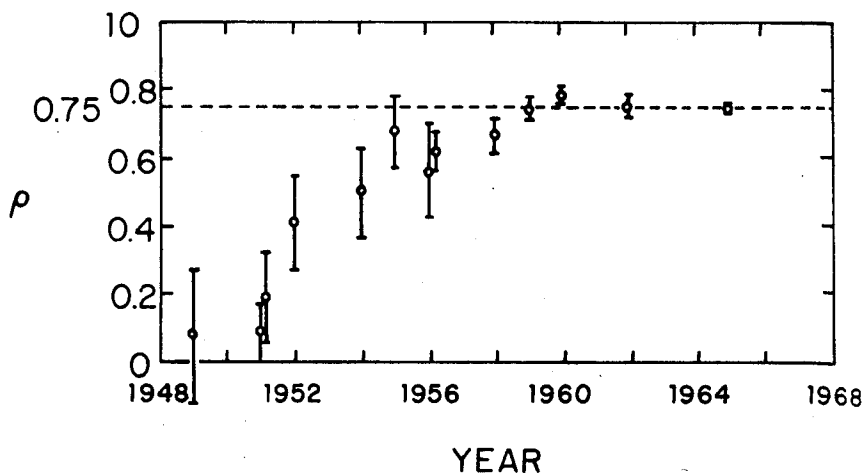


Fig. 21.2. Experimental determination of the Michel parameter ρ versus time.

It is instructive to plot the experimental value of ρ against the year when the measurement was made. As shown in Figure 21.2, historically it began with $\rho \approx 0$ and then slowly drifted upwards; only after the theoretical prediction in 1957 did it gradually become $\rho = \frac{3}{4}$. Yet, it is remarkable that at no time did the "new" experimental value lie outside the error bars of the preceding one.

(ii) When $x = 1$, the distribution (21.8) becomes

$$\frac{d^2 N_e}{dx d \cos \theta} = 1 \mp \cos \theta .$$

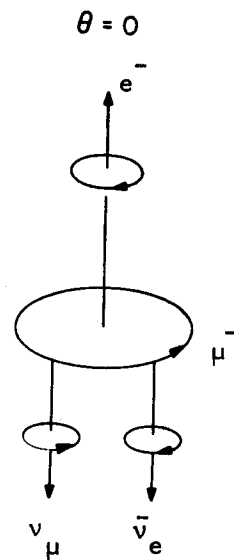
As we shall see, this expression can be derived without any actual computation. In the rest system of the muon, the momentum of e^- , \vec{p}_e , has its maximum magnitude at $x = 1$. The neutrino and anti-neutrino momenta \vec{p}_ν and $\vec{p}_{\bar{\nu}}$ must therefore be parallel to each other, but antiparallel to \vec{p}_e . Because ν is lefthanded and $\bar{\nu}$ is righthanded, when these two particles are moving in the same

direction, they transform together under a Lorentz transformation.

$$\vec{p}_\nu + \vec{p}_{\bar{\nu}} = -\vec{p}_e$$

as in (13.101), the angular distribution of $\cos \theta$.

In the μ^- decay, the forbidden direction $\theta = \pi$ is forbidden, but $\theta = 0$ is allowed. The angular distribution of e^- has to be $1 - \cos \theta$; li



FORBIDDEN

Fig. 21.3. The curled arrows in μ^- decay.

which do not require production of ν_2 , can still set a limit on the mixing angle ζ .

Hadronic weak processes set limits on right-handed currents independently of ν_R masses. In a class of models, called "manifestly" $L-R$ symmetric, the left-handed and right-handed Kobayashi-Maskawa quark mixing angles are assumed to be identical, and CP invariance is assumed to hold. In these models the K_L-K_S mass difference requires $m(W_2) > 1.6$ TeV (Ref. 6), and current-algebra analysis of $\Delta S = 1$ decays yields $\zeta \leq 0.004$, $m(W_2) > 300$ GeV for $\xi = 0$. (Ref. 7). If left-handed and right-handed mixing angles are not identical hadronic processes are consistent with $m(W_2) \geq 300$ GeV (Ref. 8). Another strong limit $\zeta < 0.005$ has been obtained in a model-dependent analysis of semileptonic weak processes, again assuming manifest $L-R$ symmetry.⁹

Figure 1 exhibits contours corresponding to 90% confi-

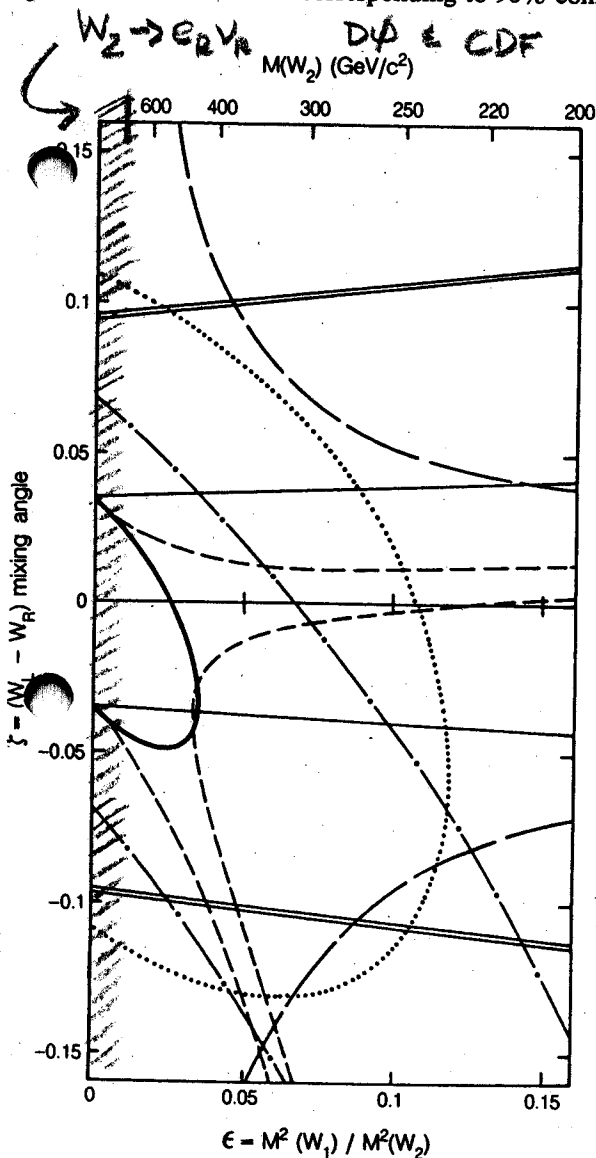


FIG. 1. Experimental 90% confidence limits on the mass-squared ratio ϵ and mixing angle ζ for the gauge bosons W_1 and W_2 . The allowed regions are those which include $\epsilon = \zeta = 0$. The bold ellipse is the combined result from the analysis presented in this paper and from our μ SR analysis (Refs. 11 and 12). The curves of the other limits are described in the text.

dence limits¹⁰ on ϵ and ζ from experiments in β decay, μ decay, and $\nu N, \bar{\nu} N$ scattering. The allowed regions contain the origin $\epsilon = \zeta = 0$, which is the $V-A$ limit. Manifest $L-R$ symmetry has been assumed. The contours from μ - and β -decay experiments have been plotted with the assumption that the right-handed neutrinos are sufficiently light not to affect the kinematics. The bold ellipse in Fig. 1 is the combined result from the analysis of the muon-decay spectrum end point opposite the μ^+ spin, presented in this paper, and from our μ SR analysis.^{11,12} The other muon-decay contours are derived from the measurement¹³ of the polarization parameter ξP_μ (dotted curve) and the Michel parameter¹⁴ ρ (solid curve). Nuclear β -decay contours are derived from the Gamow-Teller β polarization¹⁵ (dot-dashed curve); the comparison of Gamow-Teller and Fermi β polarizations¹⁶ (long-dashed curves); and the ¹⁹Ne asymmetry $A(0)$ and ft ratio,¹⁷ with the assumption of conserved vector current (short-dashed curves). The limits from the y distributions¹⁸ in $\nu N, \bar{\nu} N$ scattering (double lines) are valid irrespective of ν_R mass.

Section II of this paper discusses the properties of the muon-decay spectrum and their application to the data analysis. The beamline and experimental apparatus are discussed in Sec. III. Event reconstruction and selection are considered in Sec. IV. Data analysis and data fitting results are presented in Sec. V, and systematic errors are discussed in Sec. VI. The conclusions from the experimental result are drawn in Sec. VII.

II. MUON-DECAY SPECTRUM

The muon differential decay rate for an interaction mediated by a heavy vector boson W differs from the decay rate computed with the corresponding four-fermion contact interaction Hamiltonian by terms¹⁹ of order $(m_\mu/M_W)^2$. These terms are $\approx 10^{-6}$ for $M_W \approx 80$ GeV/ c^2 and are negligible at the present level of experimental precision. Consequently we will use the expression for the muon-decay spectrum computed for a four-fermion contact interaction. We will also assume that neutrinos are sufficiently light not to affect the kinematics. We will return to the question of massive neutrinos in Sec. VII G.

Without radiative corrections, the muon differential decay rate,²⁰ integrated over e^+ spin directions, is given by

$$\frac{d^2\Gamma}{x^2 dx d(\cos\theta)} \approx \left[(3-2x) + \left(\frac{4}{3}\rho - 1\right)(4x-3) + 12 \frac{m_e}{m_\mu} \frac{x-1}{x} \eta \right] - [(2x-1) + \left(\frac{4}{3}\delta - 1\right)(4x-3)] \xi P_\mu \cos\theta. \quad (2.1)$$

Here x is the reduced energy E_e/E_{\max} , where $E_{\max} = (m_e^2 + m_\mu^2)/(2m_\mu) = 52.83$ MeV is the maximum energy and m_e and m_μ are the particle masses. The effects of finite positron mass are neglected in the above formula but not in the analysis. The angle between the positron momentum and the muon polarization vector

P_μ in t values²¹ measured pr given th to lowest to $\epsilon = \zeta =$
The f muon-de (%) The fermion heavy int ditional correction teraction, Carlo sim method. were need The ra pure $V-$

2.0
1.8
1.6
1.4
1.2
1.0
0.8
0.6
0.4
0.2
0.0

d (events)/dx d cos θ per decay

FIG. 2. Muon-decay spectrum plotted against the angle between the positron momentum and the muon polarization vector.

This is not just a silly effort at getting a number precisely. If the gauge group of the electroweak interactions is larger than $SU(2) \times U(1)$ - more gauge bosons would be required. In particular, a RH W' is interesting as it would rationalize the lack of respect for parity.

So, W_L and W_R would presumably mix and one defines

$$\begin{aligned}
 W_1 &= \cos\theta W_L + \sin\theta W_R & = \text{observed } W \text{ boson} \\
 W_2 &= -\sin\theta W_L + \cos\theta W_R & = \text{new, unobserved}
 \end{aligned}$$

physical masses \uparrow

μ decay provides a means of testing this, which because of extreme precision, reaches to very high mass exclusion and mixing angle limits. Shown on the next page are limits from the most precise measurement at TRIUMF in Vancouver.